The contrast between defect solitons in parity–time symmetric superlattice and simple-lattice complex potentials*

Hu Su-Mei(胡素梅)[a)b)] and Hu Wei(胡 巍)[a)†]

[a)] *Laboratory of Photonic Information Technology, South China Normal University, Guangzhou* 510631, *China*
[b)] *Department of Physics, Guangdong University of Petrochemical Technology, Maoming* 525000, *China*

(Received 9 June 2011; revised manuscript received 5 August 2011)

The existence and stability of defect superlattice solitons in parity–time (PT) symmetric superlattice and simple-lattice complex potentials are reported. Compared with defect simple-lattice solitons in similar potentials, the defect soliton in superlattice has a wider stable range than that in simple-lattice. The solitons' power increases with increasing propagation constant. For the positive defect, the solitons are stable in the whole region where solitons exist in the semi-infinite gap. For the zero defect, the solitons are unstable at the edge of the band. For the negative defect, the solitons propagate with the shape of Y at low propagation constant and propagate stably at the large one.

Keywords: defect superlattice solitons, parity–time symmetry

PACS: 42.81.Dp **DOI:** 10.1088/1674-1056/21/2/024212

1. Introduction

Quite recently the light propagation in parity–time (PT) symmetry optical media has been widely studied both theoretically and experimentally.[1−6] The original motivation stems from the initial ideas of the generalization of quantum mechanics suggested by Bender *et al.*[7] With the PT symmetry complex potentials, non-Hermitian Hamitonians can have an entirely real eigenvalue spectrum.[2,5] Here the action of parity operator $\hat{P}$ is defined by the relations $\hat{p} \longrightarrow -\hat{p}$ and $\hat{x} \longrightarrow -\hat{x}$, however, that of the time operator $\hat{T}$ by $\hat{p} \longrightarrow -\hat{p}$, $\hat{x} \longrightarrow -\hat{x}$ and $\hat{\mathrm{i}} \longrightarrow -\hat{\mathrm{i}}$, here $\hat{p}$ and $\hat{x}$ respectively correspond to the momentum and position operators.[5,7] The Hamitonian $\hat{H} = \hat{p}^2/2h + V(\hat{x})$, here $V(\hat{x})$ represents complex potential. Therefore the involved real part of the PT symmetry complex potential must be an even function of position whereas the imaginary component should be odd. An interesting feature is related to spontaneous PT symmetry-breaking beyond which this class of systems can undergo an abrupt phase transition.[2,5] The system loses its PT property and as a result some of the eigenvalues become complex above the critical threshold. The origin of nonlinear switching in the PT symmetric directional couplers is related to the effect of suppression of time reversal.[8]

Defect solitons in an optical lattice are of nonlinear defect modes. Such solitons have been widely studied in the regime of photonic crystals, waveguide arrays and optically induced photonic lattices.[9−11] In particular, the defect in one-dimensional optical lattice has unique properties of solitons.[12] Defect solitons have the potential applications for the all-optical switches and routing of optical signals.[13] Soliton phenomena in superlattices have been attracting considerable attention.[14−19] Optical superlattices can be considered as regular lattices hosting a periodic chain of defects. Superlattices are fascinating because the structures exhibit collective properties not shared by either constituent and these properties can be controlled through variation of the structural parameters.[20] Defect line modes and defect solitons in PT symmetry complex potentials have been studied in Refs. [21] and [22] but these researches are limited to the simple-lattice complex potentials and the contrast between the defect solitons in the superlattices and simple-lattice PT symmetric complex potentials

*Project supported by the National Natural Science Foundation of China (Grant Nos. 10804033 and 10674050), the Program for Innovative Research (Grant No. 06CXTD005), and the Specialized Research Fund for the Doctoral Program of Higher Education of China (Grant No. 200805740002).

†Corresponding author. E-mail: huwei@scnu.edu.cn

© 2012 Chinese Physical Society and IOP Publishing Ltd

are not explored.

In this paper, we shall study the contrast between the defect solitons in defective PT symmetric superlattice and simple-lattice complex potentials. The formulation for calculating the optical propagation properties of defect solitons is given in Section 2. In Sections 3 we illustrate and discuss the results obtained. And Section 4 gives the conclusion.

2. Model

We consider optical propagation properties in self-focusing Kerr-nonlinear defective PT symmetry superlattice complex potentials.

$$\mathrm{i}\frac{\partial U}{\partial z}+\frac{\partial^2 U}{\partial x^2}+[V(x)+\mathrm{i}W(x)]U+|U|^2U=0, \quad (1)$$

where U is the slowly varying complex field envelop, x the transverse distance and z the propagation distance. $V(x)$ is the real part of PT symmetry complex potentials,

$$\begin{aligned} V(x) &= \epsilon_1 \sin^2\left(x+\frac{\pi}{2}\right) \\ &\quad + (1-\epsilon_1)\sin^2\left[2\left(x+\frac{\pi}{2}\right)\right], \\ &\quad x \le -\frac{\pi}{2},\ x \ge \frac{\pi}{2}; \\ V(x) &= (c+\epsilon_2)\sin^2\left(x+\frac{\pi}{2}\right), \\ &\quad -\frac{\pi}{2} \le x \le \frac{\pi}{2}. \end{aligned} \quad (2)$$

Here ϵ_1 represents the modulation parameter of superlattice peak strength and ϵ_2 represents the modulation parameter for defect. The constant c is introduced to make the peak strength of the defect at $\epsilon_2 = 0$ approximate to that of superlattice at a given value of ϵ_1. When $\epsilon_1 = 0.3$, $c = 0.85$, and $\epsilon_1 = 1$ is corresponding to the simple-lattice potentials. In this paper, we take $\epsilon_1 = 0.3$ for superlattice potentials. $W(x)$ is the imaginary part of PT symmetry complex potentials and we suppose

$$W(x) = W_0 \sin\left[2\left(x+\frac{\pi}{2}\right)\right]. \quad (3)$$

Different PT symmetric defect optical superlattice profiles with $\epsilon_1 = 0.3$ and $W_0 = 0.1$ are displayed in Figs. 1(a), 1(b), and 1(c). Figure 1(d) shows the Floquet–Bloch spectra of the superlattice with $\epsilon_1 = 0.3$ for different W_0, which are obtained by the plane wave expansion method. In general, the band structure of a complex lattice may be complex. However, the band diagram can be entirely real as long as the system is operated below the phase transition point (unbroken PT symmetry).[7] For the PT symmetric defective superlattice potential in Eqs. (2) and (3), we find that purely real bands are possible in the range $0 < W_0 < 0.3$. We can see from Fig. 1(d) that above the phase transition point ($W_0 = 0.4$), the band gap closes completely, so in this paper, we take $W_0 = 0.1$. From Fig. 1(d), we can see that the range of the semi-infinite gap is $\lambda > 0.505$ for $\epsilon_1 = 0.3$ and $W_0 = 0.1$.

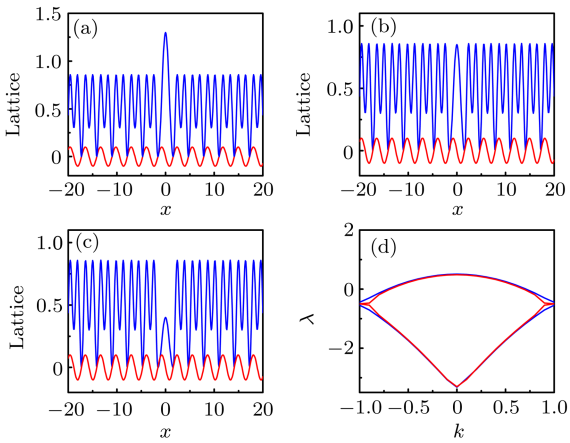


Fig. 1. (colour online) Lattice strength profile with $\epsilon_1 = 0.3$ and $W_0 = 0.1$. Blue and red lines represent real and imaginary parts of defective superlattice PT potentials, respectively: (a) $\epsilon_2 = 0.45$, (b) $\epsilon_2 = 0$, and (c) $\epsilon_2 = -0.45$; (d) bandgap structure corresponding to uniform PT superlattice with $W_0 = 0.1$ (blue line) and $W_0 = 0.4$ (red line).

We sought stationary soliton solutions to Eq. (1) in the form $U = f(x)\exp(\mathrm{i}\lambda x)$, where λ is a propagation constant and $f(x)$ is the complex periodic function satisfying the equation,

$$\lambda f = \frac{\partial^2 f}{\partial x^2} + [V(x)+\mathrm{i}W(x)]f + |f|^2 f = 0. \quad (4)$$

We numerically solve Eq. (4). To examine the stability of solitons in PT symmetry defective superlattice complex potentials, we search for the perturbed solution to Eq. (1) in the form $U(x,z) = \exp(\mathrm{i}\lambda z)\{f(x) + [g(x) - h(x)]\exp(\delta z) + [g(x)+h(x)]^*\exp(\delta^* z)\}$. Here $g(x)$, $h(x) \ll 1$, the superscript $*$ means complex conjugation. By linearizing Eq. (1), we arrive at coupled equations,

$$\begin{aligned} \delta g &= -\mathrm{i}\left[\frac{\mathrm{d}^2 h}{\mathrm{d}x^2} - \lambda h + vh - \mathrm{i}Wg + 2|f|^2 h \right. \\ &\quad \left. - \frac{1}{2}(f^2 - f^{*2})g - \frac{1}{2}(f^2 + f^{*2})h\right], \\ \delta h &= -\mathrm{i}\left[\frac{\mathrm{d}^2 g}{\mathrm{d}x^2} - \lambda g + vg - \mathrm{i}Wh + 2|f|^2 g\right. \end{aligned}$$

$$+\frac{1}{2}(f^2-f^{*2})h+\frac{1}{2}(f^2+f^{*2})g\Big].$$

These equations are solved numerically to obtain the perturbation growth rate. If $\mathrm{Re}(\delta)>0$, solitons are unstable. Otherwise, they are stable.

3. Numerical results

For the positive defect, we assume $\epsilon_2=0.45$. The power of solitons is defined as $P=\int_{-\infty}^{+\infty}|f(x)|^2\mathrm{d}x$. Figure 2(a) shows the power of solitons versus the propagation constant λ with different ϵ_1. We can see that the power of solitons increases with increasing propagation constant λ and the power of solitons in superlattice PT complex potentials is lower than that in simple-latteice PT complex potentials at the same λ. Figures 2(b) and 2(c) show the field distribution of DSUSs with different propagation constant λ, which correspond to the cases marked with circles in Fig. 2(a). Figures 2(d) and 2(e) are the field distributions of DSISs with the same propagation constant as in Figs. 2(b) and 2(c) respectively. We can see that the real parts of the field are in even symmetry and the imaginary parts are in odd symmetry for all the propagation constants λ. The field distributions of DSISs and DSUSs are homologous with large propagation constants [Figs. 2(c) and 2(e)] and they are different for low propagation constants [Figs. 2(b) and 2(d)].

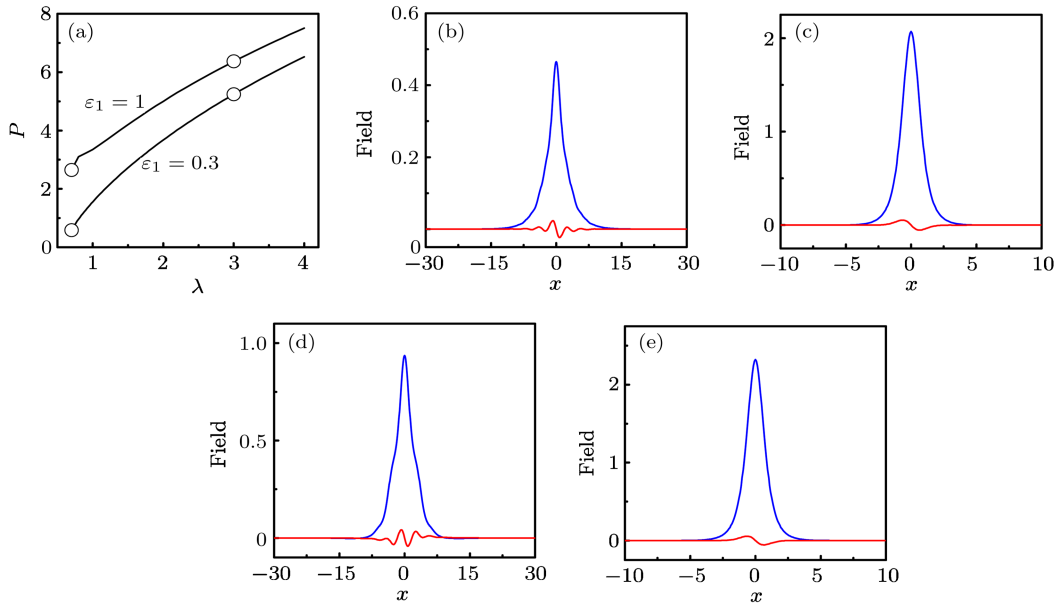


Fig. 2. (color online) For the positive defect with $\epsilon_2=0.45$, (a) power P versus propagation constant λ with different ϵ_1. (b) and (c) The field distributions of DSUSs for $\lambda=0.6$ and $\lambda=3.0$, respectively. (d) and (e) The field distributions of DSISs for $\lambda=0.6$ and $\lambda=3.0$, respectively. All of the blue lines represent the real parts of fields and red lines represent the imaginary parts of fields and all of the imaginary parts in the field profiles are multiplied by 2.

We add the solitons with 10% random-noise perturbations into the initial input when we simulate soliton propagation. Figures 3(a)–3(d) are the evolution of solitons corresponding to Figs. 2(b)–2(e). For large propagation constant λ, both the DSUSs and DSISs in PT symmetric complex potentials are stable [Figs. 3(c) and 3(d)]. For the low propagation constant λ, the DSUSs propagate stably [Fig. 3(a)], while the DSISs are divided into two parts [Fig. 3(b)]. So for the positive defect, DSUSs are stable in the whole region where solitons exist in the semi-infinite gap, which is different from the solitons in real defective superlattice potential.[14] However, the DSISs are unstable at the edge of the second band.

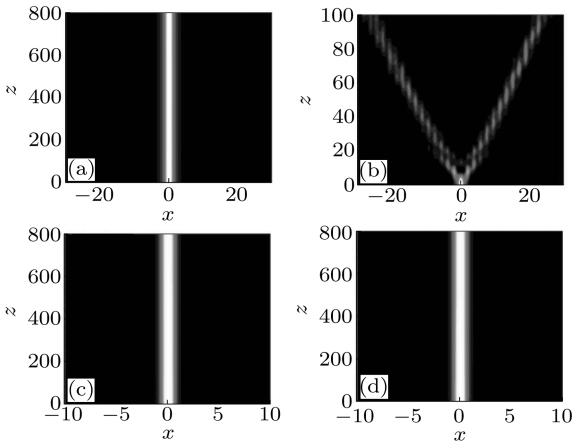


Fig. 3. (a)–(d) Evolution of solitons corresponding to Figs. 2(b)–2(e), respectively.

Figure 4(a) shows the power of solitons versus the propagation constant λ for the zero defect ($\epsilon_2 = 0$) with different ϵ_1. The power of DSUSs for the positive defect is lower than that for the zero defect. It is well known that a positive defect can be regarded as a higher index waveguide, so lower power is needed to form solitons. Figures 4(c)–4(f) show the field distributions of DSUSs and DSISs with different propagation constant λ, which are corresponding to the cases marked with circles in Fig. 4(a). We can see that all of the real parts of the field are even-symmetrical and the imaginary parts are odd-symmetrical, which are similar to the solitons for the positive defect. The imaginary parts of the fields are higher than the real parts with low propagation constant for DSISs [Fig. 4(d)]. The field distributions of DSISs and DSUSs are homologous with high propagation constant [Figs. 4(e) and 4(f)]. Figure 4(b) shows the perturbation growth rate versus propagation constant λ for DSUSs.

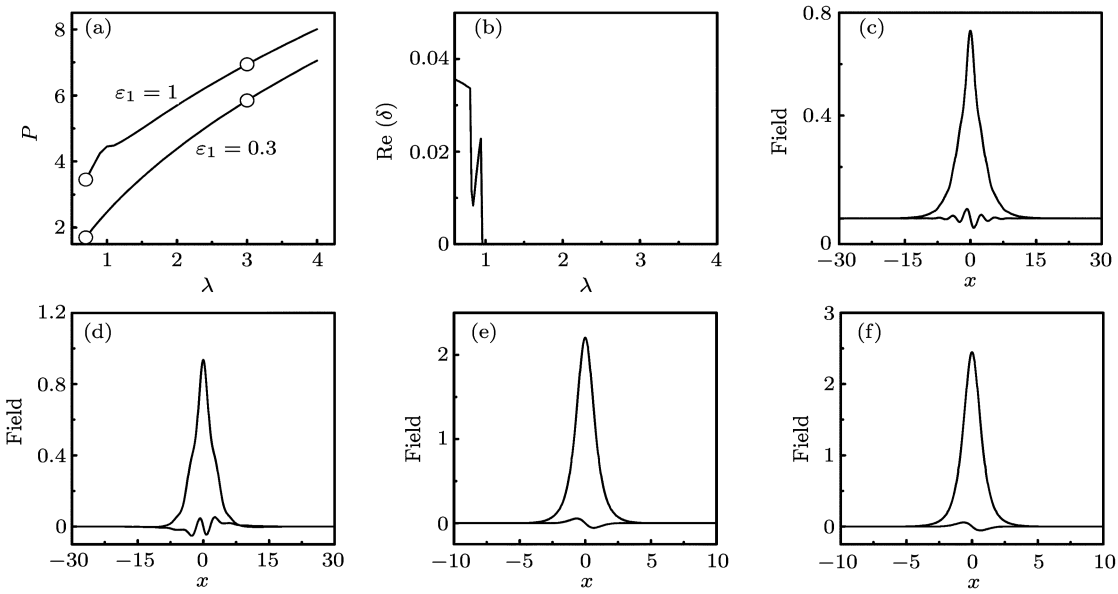


Fig. 4. For zero defect $\epsilon_2 = 0$, (a) the power P versus propagation constant λ with different ϵ_1. (b) and (c) The field distributions of DSUSs for $\lambda = 0.6$ and $\lambda = 3.0$, respectively. (d) and (e) The field distributions of DSISs for $\lambda = 0.6$ and $\lambda = 3.0$, respectively. All of the blue lines represent the real parts of fields and the red lines represent the imaginary parts of fields, all of the imaginary parts in the field profile are multiplied by 2.

Figures 5(a)–5(c) show the evolutions corresponding to Figs. 4(c)–4(f). The DSUSs propagate stably with high propagation constant λ [Fig. 5(c)]. However, at the dege of the band the DSUSs propagate stably for a certain distance then drift [Fig. 5(a)]. These are in agreement with the stable analysis in Fig. 4(b). The DSISs are unstable at the low propagation constant too and at the high propagation constant, the DSISs are stable [Figs. 5(b) and 5(d)]. So for the zero defect, DSUSs and DSISs are stable in the most of the semi-infinite gap region except for the edge of the second band.

For the negative defect, we take $\epsilon_2 = -0.45$. Figure 6(a) shows that the power of DSUSs and DSISs also increases with increasing propagation constant for the negative defect and the power of DSUSs are lower than that of DSISs with the same propagation constant, which is similar to positive defect and zero defect. However, the power of DSUSs for the negative

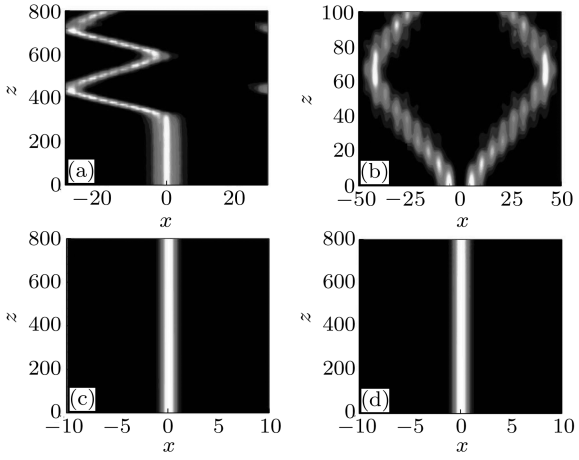


Fig. 5. (a) and (c) Evolution of DSUSs corresponding to Figs. 4(c) and 4(e) respectively. (b) and (d) Evolution of DSISs corresponding to Figs. 4(d) and 4(f) respectively.

defect is lower than that for the zero defect with the same propagation constant. This is because the negative defect acts as a lower index waveguide, more

power is needed to form solitons. Figures 6(c)–6(f) show the field distributions of DSUSs and DSISs with different propagation constant λ, which are corresponding to the cases marked by circles in Fig. 6(a). We can see that all the real parts of the field are even-symmetrical and the imaginary parts are odd-symmetrical, similar to the solitons for the positive defect and zero defect. The field distributions of DSISs and DSUSs are homologous with high propagation constant [Figs. 6(e) and 6(f)]. Figure 6(b) illustrates the perturbation growth rate versus propagation constant λ for DSUSs.

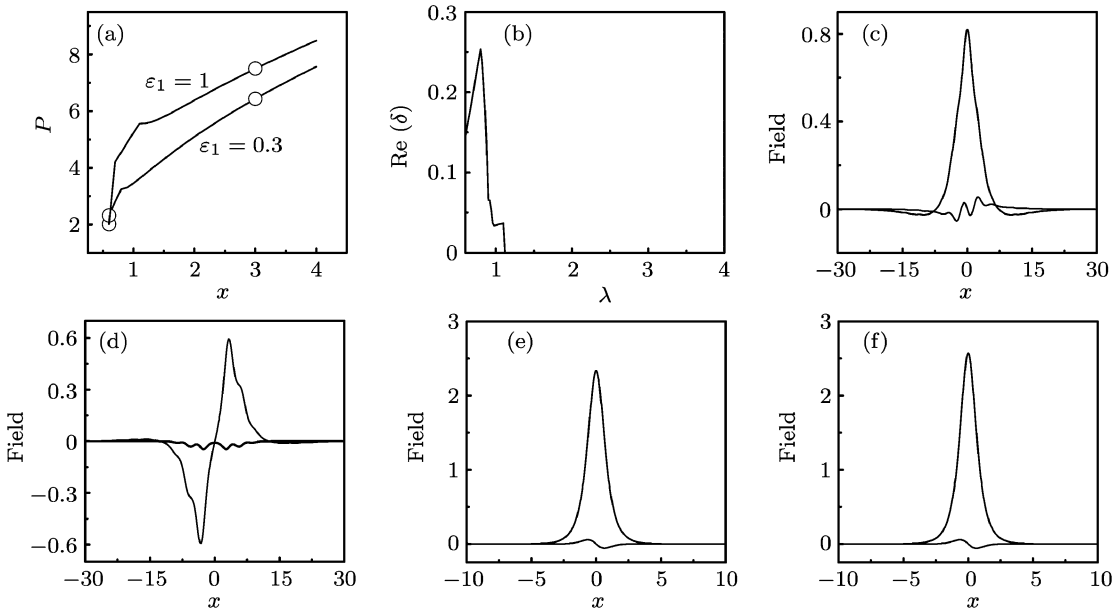


Fig. 6. For negative defect $\epsilon_2 = -0.45$, (a) the power P versus propagation constant λ with different ϵ_1. (b) and (c) The field distributions of DSUSs for $\lambda = 0.6$ and $\lambda = 3.0$, respectively. (d) and (e) The field distributions of DSISs for $\lambda = 0.6$ and $\lambda = 3.0$, respectively. All of the blue lines represent the real parts of fields and the red lines represent the imaginary parts of fields, all of the imaginary parts in the field profiles are multiplied by 2 except for (d).

Figure 7 shows the evolutions of solitons corresponding to Figs. 6(c)–6(f). The DSUSs propagate stably with high propagation constant λ [Fig. 7(c)].

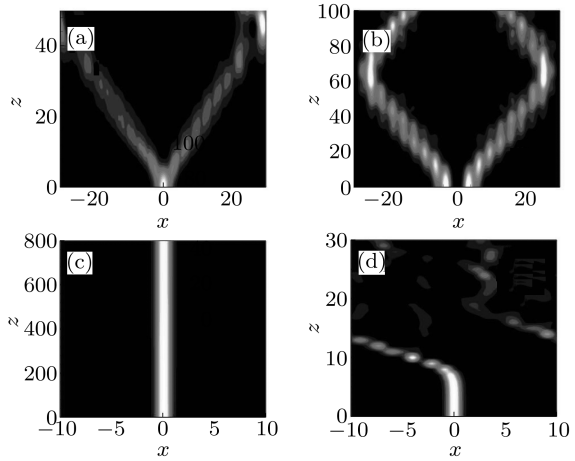


Fig. 7. (a)–(d) Evolutions of solitons corresponding to Figs. 6(c)–6(f), respectively.

However, for the low propagate constant λ the DSUSs are divided equally into two parts along the propagation direction, which emerge as in the shape of Y [Fig. 7(a)]. These are in agreement with the stable analysis in Fig. 6(b). DSISs are unstable not only at the low propagation constant but also at large propagation constant. [Figs. 7(b) and 7(d)].

4. Conclusions

In conclusion, we have compared the defect solitons supported by parity–time symmetric defective superlattice and simple-lattice complex potentials. Solitons' power increases with increasing propagation constant λ and the power of DSUSs is lower than that of DSISs for the same propagation constant. For the positive defect, the DSUSs are stable in the whole region where solitons exist in the semi-infinite gap, but the DSISs are unstable at the edge of the second band. For the zero defect, the DSUSs are unstable at the dege of the band and stable at large propagation constant. For the negative defect, the DSUSs propagate in the shape of Y at low propagation constant and propagate stably at high propagation constant, while DSISs are unstable not only at the low propagate constant but also at the large propagate constant.

References

[1] Makris K G, Ganainy R EI, Christodoulides D N and Musslimani Z H 2010 *Phys. Rev.* A **81** 06387

[2] Bendix O, Fleischmann R, Kottos T and Shapiro B 2009 *Phys. Rev. Lett.* **103** 030402

[3] Jin L and Song Z 2009 *Phys. Rev.* A **80** 052107

[4] West C T, Kottos T and Prosen T 2010 *Phys. Rev. Lett.* **104** 054102

[5] Musslimani Z H, Makris K G, Ganainy R EI and Christodoulides D N 2008 *Phys. Rev. Lett.* **100** 030402

[6] Guo A, Salamo G J, Duchesne D, Morandotti R, Volatier-Ravat M, Imez V, Siviloglou G A and Christodoulides D N 2009 *Phys. Rev. Lett.* **103** 093902

[7] Bender C M, Brody D C and Jones H F 2002 *Phys. Rev. Lett.* **27** 270401

[8] Sukhorukov A A, Xu Z Y and Kivshar Y S 2010 *Phys. Rev. Lett.* **82** 043818

[9] Yaroslav F Y, Kartashov V, Vysloukh V A and Torner L 2008 *Phys. Rev.* A **78** 013847

[10] Li Y Y, Pang W, Chen Y Z, Yu Z Q and Zhang H Y 2009 *Phys. Rev.* A **80** 043824

[11] Brazhnyi V A, Konotop V V and Perez-Garcia V M 2006 *Phys. Rev. Lett.* **96** 060403

[12] Fedele F, Yang J and Chen Z 2005 *Phys. Rev. Lett.* **30** 1506

[13] Campbell D K, Flach S and Kivshar Y S 2004 *Phys. Today* **57** 43

[14] Chen W H, He Y J and Wang H Z 2007 *Opt. Express* **22** 14498

[15] Zhang Z Y and Xiong S J 1997 *Phys. Rev.* B **55** 10302

[16] Alekseev K N, Berman G P, Campbell D K, Cannon E H and Cargo M C 1996 *Phys. Rev.* B **54** 10625

[17] Porter M A, Kevrekidis P G, Carretero-Gonzalez R and Frantzeskakis D J 2006 *Phys. Lett.* A **352** 210

[18] Ghulinyan M, Oton C J, Gaburro Z, Pavesi L, Toninelli C and Wiersma D S 2005 *Phys. Rev. Lett.* **94** 127401

[19] Dreisow F, Szameit A, Heinrich M, Pertsch T, Nolte S, Unnermann A T and Longhi S 2009 *Phys. Rev. Lett.* **102** 076802

[20] Chen W and Mill D L 1987 *Phys. Rev. Lett.* **58** 160

[21] Zhou K Y, Guo Z Y, Wang J C and Liu S T 2010 *Opt. Lett.* **35** 172928

[22] Hang W and Wang J D 2011 *Opt. Express* **19** 4030